

Optimization of Nanoliposomes Production using a Coaxial Jet Mixer: a Response Surface Modeling Approach

Diego Caccavo^{a,b,*}, Raffaella De Piano^a, Luca Broegg^b, Anna Angela Barba^{b,c}, Gaetano Lamberti^{a,b}

^aDipartimento di Ingegneria Industriale, Università degli Studi di Salerno, Fisciano (SA)

^bEST SrL, via Circumvallazione 39, Avellino (AV)

^cDipartimento di Farmacia, Università degli Studi di Salerno, Fisciano (SA)

dcaccavo@unisa.it

Liposomes are vesicular structures capable of encapsulating and delivering active pharmaceutical ingredients or other compounds. A thorough understanding of their physical properties is essential for optimizing their application potential. In this work, liposomes were produced using ethanol, with phosphatidylcholine from soy lecithin processed via a coaxial jet mixer. The study investigated the effect of key operating parameters—ethanol flow rate, water flow rate, and phosphatidylcholine concentration—on four experimental responses: Z-Average, Polydispersity Index (PDI), Main Intensity Peak Size, and Zeta Potential. A Box-Behnken Design (BBD) was employed to optimize the experimental plan, minimizing the number of trials compared to a full factorial design. Measurements performed using a Zetasizer enabled the development of predictive models for the selected responses. Modeling results, based on a univariate analysis and a top-down approach, showed that within the explored parameter range, Z-Average was primarily influenced by the inner flow rate and phosphatidylcholine concentration. These parameters also significantly affected the Zeta Potential, while water flow rate had the least impact on the responses. To achieve smaller liposomes, the results indicate the need for low phosphatidylcholine concentrations combined with high inner flow rates.

1. Introduction

Liposomes are vesicles composed of one or more phospholipid bilayers surrounding an aqueous core, widely used as carriers for hydrophilic and hydrophobic substances in pharmaceutical, cosmeceutical, and food applications due to their biocompatibility and structural similarity to biological membranes. Traditional liposome production techniques, including thin film hydration, reverse-phase evaporation, and ethanol injection, remain popular; however, they often face limitations related to reproducibility, scalability, and precise control of particle size and distribution (Andra et al., 2022, Lombardo and Kiselev, 2022). In recent years, advanced continuous-flow methods have emerged to overcome these limitations, including microfluidic strategies and coaxial jet mixers, which are particularly promising (Jahn et al., 2010, Caccavo et al., 2023, Lim et al., 2014, Bochicchio et al., 2018). These mixers enable rapid and controlled nanoprecipitation by mixing a lipid solution in an organic solvent (such as ethanol) with an antisolvent (usually water), facilitating rapid lipid self-assembly and vesicle formation under highly reproducible hydrodynamic conditions (Caccavo et al., 2023, Lim et al., 2014). To fully exploit the advantages of coaxial jet mixers, it is crucial to understand the impact of key operating parameters — such as solvent and antisolvent flow rates, and lipid concentration — on liposome characteristics including particle size, polydispersity, and zeta potential. Computational fluid dynamics (CFD) combined with nanoprecipitation models provide detailed mechanistic insights, yet these approaches often require complex modeling and significant computational resources. For example, advanced works such as those by Gavi et al. (Gavi et al., 2007) and Saad and Prud'homme (Saad and Prud'homme, 2016) rely on detailed descriptions of turbulent mixing, micromixing scales, and nucleation-growth kinetics to model nanoparticle formation and liposome self-assembly. While these approaches offer deep mechanistic understanding, they involve high-dimensional parameter spaces, fluid dynamic simulations, and nontrivial coupling between transport and

thermodynamic phenomena. Alternatively, statistical approaches such as Design of Experiments (DOE) and Response Surface Methodology (RSM) have proven highly effective for systematic exploration of process parameters. These methods allow for reduced experimental workload, identification of main and interaction effects, and development of regression-based predictive models without requiring detailed phenomenological knowledge. For instance, Buttitta et al. (Buttitta et al., 2024) optimized liposome production in a micromixer device using a response surface methodology-based design, evaluating cholesterol concentration, total flow rate, and flow rate ratio as critical process parameters. Kastner et al. (Kastner et al., 2014) investigated process and formulation parameters influencing liposome characteristics using a response surface methodology approach based on a quadratic model, applied to a microfluidic mixer using an ethanol–water system. Lindsay et al. (Lindsay et al., 2024) implemented a DOE-based experimental plan combined with machine learning to assess the influence of total flow rate, flow rate ratio, lipid concentration, lipid type, solvent, buffer composition, and temperature on liposome formation in a micromixer-based microfluidic system. López et al. (López et al., 2020) used RSM to study the effects of flow rate and phospholipid concentration on size and encapsulation efficiency in a Periodic Disturbance Mixer-based microfluidic device. Rebollo et al. (Rebollo et al., 2022) applied a Design of Experiments (DOE) approach combined with Artificial Neural Networks (ANN) to model the influence of cholesterol concentration, total flow rate, and flow rate ratio on vesicle properties produced in a microfluidic chip. Yenduri et al. (Yenduri et al., 2022) applied a DOE within a Quality by Design (QbD) framework to optimize liposomal formulations using a modified ethanol injection method with a coaxial jet in co-flow—closely resembling the setup used in this work. Their study focused on CMAs such as PG content, lipid chain length, cholesterol, and aqueous medium, and CPPs including aqueous flow rate and formation temperature, with ethanol flow fixed at 40 mL/min. Compared to their lower flow rates, the present study explores a broader range, incorporating both ethanol (X_1) and water (X_2) flow rates and PC concentration (X_3) as factors. A Box-Behnken design was employed to efficiently model multiple liposome attributes and support process optimization through predictive modeling.

The objective of the present study is thus to systematically investigate the influence of ethanol flow rate (solvent), water flow rate (antisolvent), and phosphatidylcholine concentration on the physicochemical properties—Z-Average, Polydispersity Index (PDI), Main Intensity Peak Size (MIPS), and Zeta Potential—of unloaded liposomes produced by a coaxial turbulent jet mixer. A Box-Behnken experimental design was employed to minimize the number of experiments while maintaining statistical rigor, enabling the construction of linear predictive models to assess the significance and impact of each factor.

2. Materials and methods

2.1 Materials

Soy lecithin PWD E 322 was purchased from ACEF S.p.A. (Fiorenzuola d'Arda, Italy) and used as phospholipid source. Absolute ethanol ($\geq 99.8\%$) was purchased from Carlo Erba Reagents (Milan, Italy) and used as the organic solvent. Deionized water was used as the antisolvent for liposome formation and for dilution prior to measurement.

2.2 Phospholipids extraction from soy lecithin

To extract phospholipids from the soy lecithin, a 1.5:1 ethanol-to-lecithin weight ratio was employed. The mixture was stirred at room temperature (25 °C) for 24 hours to enhance lipid solubilization. After extraction, the suspension was centrifuged for 15 minutes to separate the solid residue. A 3 mL aliquot of the supernatant was transferred onto a pre-weighed Petri dish and placed in a ventilated oven at 40 °C for 30 minutes to remove residual ethanol. The dried residue, corresponding to extracted phospholipids—predominantly phosphatidylcholine (PC), the most abundant and ethanol-soluble component of soybean lecithin—was weighed to calculate the extraction yield (about 15%). This procedure was repeated three times with independent samples to improve reproducibility. Final concentrations were adjusted by progressive dilution of the concentrated extract in ethanol to match the desired values for subsequent experimental runs.

2.3 Nanoliposomes production

Liposomes were produced using a coaxial turbulent jet mixer equipped with an inner 23G stainless steel needle and an outer 9G stainless steel tube. The ethanolic lipid solution was pumped through the inner needle (solvent stream), while deionized water was simultaneously delivered through the outer tube (antisolvent stream). Flow rates were controlled using two separate high-precision dosing pumps. Stainless steel 316 tubing and dampeners (Iannone et al., 2022) were employed to ensure stable and pulsation-free flow.

Mixing occurred at the needle outlet, where the inner solvent jet met the outer water stream. The resulting hydrodynamic interaction promoted rapid mixing and the formation of supersaturation zones, triggering

phospholipid nanoprecipitation and subsequent liposome self-assembly. The emerging liposomal suspension was collected in a beaker.

2.4 Nanoliposomes characterization

Size, PDI, and zeta potential were measured at 25 °C using a NanoZetasizer Pro Lab Red (Malvern Panalytical, UK). Undiluted samples were analyzed in triplicate using disposable cuvettes (size/PDI) and folded capillary cells (zeta potential).

2.5 Experimental Design (Box-Behnken Design)

To investigate the influence of process parameters on liposome characteristics, a Design of Experiments (DOE) approach based on a Box-Behnken Design (BBD) was adopted. This RSM-based design allows efficient modeling of nonlinear effects and interactions among factors while limiting the number of experimental runs compared to full factorial designs. Three critical process parameters (CPPs) were selected as independent variables: ethanol flow rate (Q_{inner} : X_1): 18, 36, and 60 mL/min; water flow rate (Q_{outer} : X_2): 180, 360, and 600 mL/min; phospholipid concentration (C_{PL} : X_3): 25, 50, and 75 g/L. These factors were investigated at three levels (low, -1; medium, 0; high, +1) and combined in a BBD matrix to assess their effect on four liposome properties: Z-Average size (Y_1), Polydispersity Index (PDI) (Y_2), Main Intensity Peak Size (MIPS) (nm) (Y_3), and Zeta Potential (mV) (Y_4). The summary of Factors and Responses is in Table 1.

2.6 Statistical Modeling and Data Analysis

A univariate modeling strategy was employed to analyze the influence of each critical process parameter (CPP) on the selected liposome characteristics. Multiple linear regression (MLR) models were fitted using MATLAB R2023a (MathWorks Inc.), adopting various formulations including first-order (linear), interaction (linear with interactions), and second order (quadratic) polynomial models. Terms included in the models were: linear (X_1 , X_2 , X_3), two-factor interactions (e.g., X_1X_2), and quadratic terms (e.g., X_1^2).

Model quality was assessed based on the following metrics: R^2 (coefficient of determination), which indicates how well the model fits the data (higher is better); Adjusted R^2 , which corrects R^2 for the number of predictors (higher is better); AICc (corrected Akaike Information Criterion), which balances model fit and complexity (lower is better); PRESS (Prediction Error Sum of Squares), which is obtained through leave-one-out cross-validation (lower is better). Although the models were not externally validated using independent datasets, their predictive performance was internally assessed through the PRESS statistic.

The overall significance of each model was evaluated using Analysis of Variance (ANOVA). This test determines whether the model provides a significantly better fit to the data than a model with no predictors, based on the F-statistic and its associated p-value. A significant p-value (typically < 0.05) indicates that the model explains a significant portion of the variance in the response variable. In addition, ANOVA was also used to assess the significance of each individual model term (main effects, interactions, and quadratic components). Terms with p-values below 0.05 were considered statistically significant and were retained in the final, reduced models.

Table 1. Box-Behnken experimental matrix showing the combinations of process parameters and the corresponding responses (mean \pm standard deviation).

#	Factors						Responses			
	Q_{inner} [mL/min]		Q_{outer} [mL/min]		C_{PL} [g/L]		Z-average [nm]	PDI [-]	MIPS [nm]	Z-potential [mV]
	X_1	X_2	X_3	Y_1	Y_2	Y_3	Y_4			
	Value	Level	Value	Level	Value	Level				
1	36	0	360	0	50	0	26,61 \pm 6,58	0,49 \pm 0,68	51,24 \pm 2,74	-60,41 \pm 4,84
2	60	+1	600	+1	50	0	25,65 \pm 6,58	0,45 \pm 0,03	47,23 \pm 6,76	-60,52 \pm 10,82
3	18	-1	180	-1	50	0	31,61 \pm 6,61	0,74 \pm 0,22	62,96 \pm 5,74	-65,61 \pm 10,31
4	18	-1	600	+1	50	0	29,14 \pm 1,27	0,56 \pm 0,13	50,41 \pm 1,18	-42,09 \pm 8,83
5	60	+1	180	-1	50	0	23,23 \pm 1,75	0,54 \pm 0,00	66,5 \pm 4,27	-72,55 \pm 1,53
6	18	-1	360	0	25	-1	41,96 \pm 10,11	0,35 \pm 0,04	71,19 \pm 3,55	-32,76 \pm 4,47
7	60	+1	360	0	25	-1	11,33 \pm 1,93	0,67 \pm 0,10	44,67 \pm 7,06	-37,7 \pm 1,91
8	36	0	180	-1	25	-1	17,82 \pm 4,09	0,51 \pm 0,00	49,64 \pm 7,28	-38,63 \pm 2,70
9	36	0	600	+1	25	-1	12,92 \pm 1,22	0,82 \pm 0,17	43,18 \pm 10,82	-30,83 \pm 4,57
10	18	-1	360	0	75	+1	53,29 \pm 3,08	0,48 \pm 0,06	81,28 \pm 5,62	-48,34 \pm 9,29
11	60	+1	360	0	75	+1	36,73 \pm 0,82	0,49 \pm 0,17	64,24 \pm 4,29	-55,57 \pm 19,81
12	36	0	180	-1	75	+1	45,58 \pm 3,19	0,44 \pm 0,03	71,02 \pm 11,31	-60,09 \pm 8,96
13	36	0	600	+1	75	+1	33,02 \pm 1,77	0,54 \pm 0,03	52,64 \pm 1,96	-46,13 \pm 4,09

3. Results and discussion

All produced vesicles exhibited Z-average diameters below 60 nm and main intensity peak sizes (MIPS) between approximately 43 and 81 nm, confirming that the obtained structures fall within the range typically associated with small unilamellar vesicles (SUVs), 20-100 nm (Yang et al., 2011). The negative Z-potential values (ranging from approximately -30 to -73 mV) suggest good electrostatic stability across all formulations. Polydispersity Index (PDI) values were generally moderate (0.35–0.82), with most samples below the threshold of 0.5, indicating acceptable to good homogeneity of size distribution. Notably, higher lipid concentrations and lower flow rates appeared to result in larger liposomes and slightly broader size distributions, consistent with the behavior expected in antisolvent precipitation systems.

3.1 Main Intensity Peak Size (Y_3) response

Among the four considered responses, the Main Intensity Peak Size (MIPS, Y_3) was selected to demonstrate in detail the entire model selection procedure, following a top-down approach. This response was chosen as representative due to its relevance and variability. While the full selection steps are only shown for MIPS, similar procedures were followed for the remaining responses, for which only the final models will be reported.

The Main Intensity Peak Size (MIPS) was analyzed from the intensity-based size distribution of dynamic light scattering (DLS) measurements. A top-down modeling strategy was adopted to compare multiple model structures and identify the optimal formulation.

Table 2. P-values for model terms across model structures for MIPS (Y_3).

Term	Quadratic	Linear plus Interactions	Linear (no interactions)	Custom 1	Custom 2
X_1	0.22	0.14	0.076	—	0.15
X_2	0.066	0.019	0.0047	0.0084	0.016
X_3	0.12	0.057	0.023	0.037	—
$X_1 \times X_2$	0.90	0.88	—	—	—
$X_1 \times X_3$	0.65	0.60	—	—	—
$X_2 \times X_3$	0.68	0.63	—	—	—
X_1^2	0.45	—	—	—	—
X_2^2	0.96	—	—	—	—
X_3^2	0.35	—	—	—	—

Analysis of the parameter significance indicated that the linear model without interactions was the most suitable, retaining all three variables (X_1 , X_2 , X_3) with p-values below the typical significance threshold ($p < 0.05$). Custom models excluding X_1 or X_3 worsened the significance of the remaining parameters. Model performance metrics are summarized in Table 3.

Table 3. Model comparison for MIPS (Y_3): higher R^2/R^2 adj., lower AICc and PRESS indicate better fit.

Model	R^2 (↑)	R^2 adj. (↑)	AICc (↓)	PRESS (↓)
Quadratic	0.86	0.42	206.32	5180.12
Linear plus interactions	0.76	0.52	119.25	1877.89
Linear (no interactions)	0.74	0.65	97.08	988.13
Custom 1 (X_2 , X_3)	0.62	0.55	97.52	1110.18
Custom 2 (X_1 , X_2)	0.52	0.42	100.65	1463.43

Thus, the final predictive model selected for Y_3 (MIPS) was the linear with no interaction:

$$Y_3 = 72,36 - 0,25 X_1 - 0,046 X_2 + 0,29 X_3 \quad (1)$$

The model yielded an F-statistic of approximately 8.48 and a model p-value of 0.0055, confirming its overall statistical significance. Therefore, the model is appropriate for describing the experimental data.

The plots in Figure 1 illustrate how the MIPS varies as a function of the inner flow rate (X_1 , ethanol) and phosphatidylcholine concentration (X_3) under fixed water flow conditions (X_2). A clear trend emerges across all conditions: MIPS decreases with increasing X_1 and increases with increasing X_3 . This suggests that higher ethanol flow rates and lower lipid concentrations promote the formation of smaller liposomes. Notably, at the highest water flow rate (600 mL/min), the predicted MIPS values are generally lower compared to other conditions. This, in lines with the findings of Yenduri et al. (Yenduri et al., 2022), may be attributed to the more efficient mixing and higher dilution rate of the solvent at high antisolvent flow, which enhances supersaturation and accelerates nucleation, resulting in smaller liposome sizes.

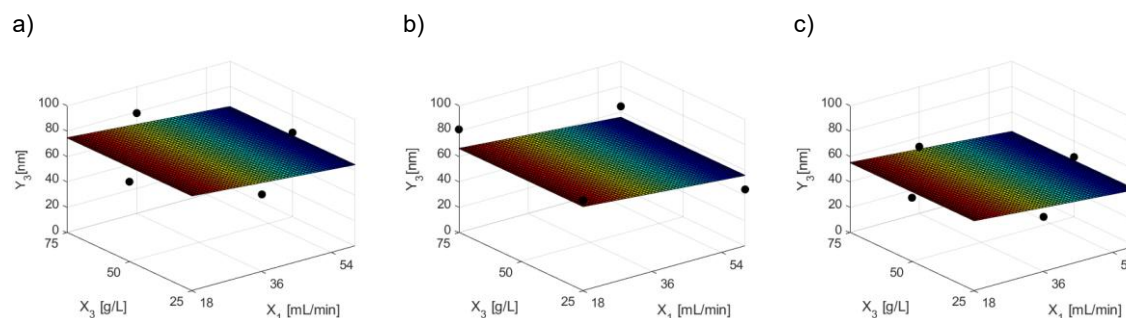


Figure 1. Response surfaces obtained from the linear model for Main Intensity Peak Size (MIPS, Y_3) at different water flow rates (X_2): a) $X_2 = 180$ mL/min, b) $X_2 = 360$ mL/min, c) $X_2 = 600$ mL/min.

3.2 Predictive Modeling of Z-Average (Y_1), PDI (Y_2), and Zeta Potential (Y_4)

Following a procedure analogous to the one detailed for Y_3 (MIPS), predictive models were developed for the remaining three responses: Z-Average (Y_1), Polydispersity Index (PDI, Y_2), and Zeta Potential (Y_4). For brevity, only the final selected equations are reported below:

$$Y_1 = 21,57 - 0,34 X_1 + 0,42 X_3 \quad (2)$$

$$Y_2 = 0,97 + 0,0038 X_1 - 0,001 X_2 - 0,0088 X_3 + 0,0000136 X_2 X_3 \quad (3)$$

$$Y_4 = 14,94 - 0,41 X_1 - 0,079 X_2 + 2,26 X_3 + 0,0014 X_1 X_2 - 0,019 X_3^2 \quad (4)$$

The quality of the selected models for these responses is summarized in Table 4, highlighting their statistical soundness and predictive reliability.

Table 4. Goodness-of-fit metrics for selected models: higher R^2/R^2 adj. (\uparrow), lower AICc and PRESS (\downarrow) indicate better models.

Model for	R^2 (\uparrow)	R^2 adj. (\uparrow)	AICc (\downarrow)	PRESS (\downarrow)
Y_1	0,7	0,64	94,21	1021,37
Y_2	0,91	0,86	-30,23	0,049
Y_4	0,975	0,96	77,26	116,88

In terms of Z-average (Y_1), the model reveals a negative dependence on X_1 (solvent flow rate) and a positive dependence on X_3 (lipid concentration). This implies that lower solvent flow rates and higher phospholipid concentrations tend to increase the hydrodynamic diameter of liposomes. In the present work the antisolvent flow rate (X_2) did not significantly influence Z-average (Y_1). This contrasts with findings on MIPS (Y_3): several samples showed a secondary intensity peak at 3–5 nm, likely due to micelles, aggregates, or measurement artifacts. Although DLS overweights larger particles, minor populations can still influence the Z-Average (Y_1), reducing its reliability. However, the main peak consistently represented the majority of scattering intensity (>70%), supporting the use of MIPS as a more robust indicator of dominant vesicle size. Thus, while Y_1 was modeled, its interpretation requires caution in multipopulation systems.

The PDI (Y_2) was mildly but significantly influenced by all investigated factors. Lower values were associated with higher phosphatidylcholine concentration (X_3) and antisolvent flow rate (X_2), while the solvent flow rate (X_1) had a negligible effect. The $X_2 \cdot X_3$ interaction further contributed to reducing PDI. However, due to the presence of multiple particle populations—as indicated by the particle size distribution—PDI should be considered only partially reliable in describing the true uniformity of the system.

The predictive model for Zeta Potential (Y_4) highlights a strong positive influence of phosphatidylcholine concentration (X_3), indicating that increasing the amount of lipid enhances the electrostatic stability of the liposomes. This behavior is expected, as higher PC content promotes the formation of well-defined bilayers with greater surface charge density, resulting in more negative zeta potential values and improved colloidal stability.

4. Conclusions

This study demonstrated the feasibility of producing nanoliposomes using a coaxial jet mixer and highlighted the potential of Response Surface Methodology (RSM) for optimizing key process parameters. A Box-Behnken Design enabled the modeling of liposome characteristics—Z-Average, Polydispersity Index (PDI), Main Intensity

Peak Size (MIPS), and Zeta Potential—as functions of ethanol flow rate (X_1), water flow rate (X_2), and phosphatidylcholine concentration (X_3). The main findings can be summarized as follows: smaller vesicles (MIPS down to ~43 nm) were obtained at high ethanol flow rates and low phosphatidylcholine concentrations, with X_2 (water flow rate) enhancing size reduction only for MIPS. The Z-Average (Y_1) showed a similar trend to MIPS with respect to X_1 and X_3 , but was not significantly affected by X_2 , probably due to measurement biases from minor sub-populations (~3–5 nm). The PDI (Y_2) was moderately reduced by increasing X_2 and X_3 , suggesting improved uniformity under high dilution and lipid-rich conditions. The Zeta Potential (Y_4) became more negative with increasing phosphatidylcholine concentration (up to -73 mV), indicating enhanced colloidal stability. Overall, the predictive models showed good statistical reliability, and the results confirm that coaxial jet mixers, coupled with statistically optimized formulations, offer a promising and scalable platform for producing stable nanoliposomes with tunable properties.

References

- Andra, V. V. S. N., Pammi, S. V. N., Bhatraju, L. V. K. P. & Ruddaraju, L. K. 2022. A Comprehensive Review On Novel Liposomal Methodologies, Commercial Formulations, Clinical Trials And Patents. *Bionanoscience*, 12, 274-291.
- Bochicchio, S., Dalmoro, A., Bertoncin, P., Lamberti, G., Moustafine, R. & Barba, A. 2018. Design And Production Of Hybrid Nanoparticles With Polymeric-Lipid Shell-Core Structures: Conventional And Next-Generation Approaches. *Rsc Advances*, 8, 34614-34624.
- Buttitta, G., Bonacorsi, S., Barbarito, C., Moliterno, M., Pompei, S., Saito, G., Oddone, I., Verdone, G., Secci, D. & Raimondi, S. 2024. Scalable Microfluidic Method For Tunable Liposomal Production By A Design Of Experiment Approach. *International Journal Of Pharmaceutics*, 662.
- Caccavo, D., Lamberti, G. & Barba, A. A. 2023. Coaxial Injection Mixer For The Continuous Production Of Nanoparticles. *Chemical Engineering Transactions*, 100, 301-306.
- Gavi, E., Rivautella, L., Marchisio, D., Vanni, M., Barresi, A. & Baldi, G. 2007. Cfd Modelling Of Nano-Particle Precipitation In Confined Impinging Jet Reactors. *Chemical Engineering Research & Design*, 85, 735-744.
- Iannone, M., Caccavo, D., Barba, A. A. & Lamberti, G. 2022. A Low-Cost Push–Pull Syringe Pump For Continuous Flow Applications. *HardwareX*, 11, E00295.
- Jahn, A., Stavis, S. M., Hong, J. S., Vreeland, W. N., Devoe, D. L. & Gaitan, M. 2010. Microfluidic Mixing And The Formation Of Nanoscale Lipid Vesicles. *Acs Nano*, 4, 2077-87.
- Kastner, E., Kaur, R., Lowry, D., Moghaddam, B., Wilkinson, A. & Perrie, Y. 2014. High-Throughput Manufacturing Of Size-Tuned Liposomes By A New Microfluidics Method Using Enhanced Statistical Tools For Characterization. *International Journal Of Pharmaceutics*, 477, 361-368.
- Lim, J.-M., Swami, A., Gilson, L. M., Chopra, S., Choi, S., Wu, J., Langer, R., Karnik, R. & Farokhzad, O. C. 2014. Ultra-High Throughput Synthesis Of Nanoparticles With Homogeneous Size Distribution Using A Coaxial Turbulent Jet Mixer. *Acs Nano*, 8, 6056-6065.
- Lindsay, S., Tumolva, O., Khamiakova, T., Coppenolle, H., Kovarik, M., Shah, S., Holm, R. & Perrie, Y. 2024. Can We Simplify Liposome Manufacturing Using A Complex Doe Approach? *Pharmaceutics*, 16.
- Lombardo, D. & Kiselev, M. A. 2022. Methods Of Liposomes Preparation: Formation And Control Factors Of Versatile Nanocarriers For Biomedical And Nanomedicine Application. *Pharmaceutics*, 14.
- López, R. R., Ocampo, I., Sánchez, L. M., Alazzam, A., Bergeron, K. F., Camacho-León, S., Mounier, C., Stiharu, I. & Nerguizian, V. 2020. Surface Response Based Modeling Of Liposome Characteristics In A Periodic Disturbance Mixer. *Micromachines (Basel)*, 11.
- Rebollo, R., Oyoun, F., Corvis, Y., El-Hammadi, M. M., Saubamea, B., Andrieux, K., Mignet, N. & Alhareth, K. 2022. Microfluidic Manufacturing Of Liposomes: Development And Optimization By Design Of Experiment And Machine Learning. *Acs Appl Mater Interfaces*, 14, 39736-39745.
- Saad, W. & Prud'homme, R. 2016. Principles Of Nanoparticle Formation By Flash Nanoprecipitation. *Nano Today*, 11, 212-227.
- Yang, F., Jin, C., Jiang, Y., Li, J., Di, Y., Ni, Q. & Fu, D. 2011. Liposome Based Delivery Systems In Pancreatic Cancer Treatment: From Bench To Bedside. *Cancer Treat Rev*, 37, 633-42.
- Yenduri, G., Costa, A. P., Xu, X. & Burgess, D. J. 2022. Impact Of Critical Process Parameters And Critical Material Attributes On The Critical Quality Attributes Of Liposomal Formulations Prepared Using Continuous Processing. *Int J Pharm*, 619, 121700.